

## Effects of interference grid on melt jet breakup and particle size distribution: MATE-MM-1 & 2 test cases

Mayank Modak<sup>a</sup>, Hyun Sun Park<sup>a\*</sup>, Evidente Ralph Carlo<sup>a</sup>, Woo Hyun Jung<sup>a</sup>, Yu Jung Choi<sup>b</sup>, and Mi Ro Seo<sup>b</sup>

<sup>a</sup>Division of Advanced Nuclear Engineering, POSTECH, 77 Cheongam-Ro, Nam-Gu, Pohang 790-784, Gyeongbuk, Republic of Korea

<sup>b</sup>Korea Hydro and Nuclear Power Co., Ltd., 1655, Bulguk-ro, Gyeongju-si, 38120 Gyeongbuk, Republic of Korea

\*Corresponding author E-mail: [hejsunny@postech.ac.kr](mailto:hejsunny@postech.ac.kr)

### 1. Introduction

In a scenario of severe accident in Light Water Reactors (LWRs) leads to major core damage and its subsequent melting. This molten core will eventually flow into the lower plenum of the reactor vessel. In case of insufficient cooling, the vessel wall will be damaged causing breach by high temperature melt which will be released into the reactor cavity. In the wet cavity strategy, the discharged high temperature corium can be adequately cooled by low-temperature coolant water. This fuel-coolant interaction (FCI) will allow the corium to break and settle on the bottom of the reactor cavity forming a porous debris bed. For adequate assessment of coolability of relocated corium, it is necessary to thoroughly understand the relevant processes of debris bed formation, including melt jet breakup and particle sedimentation, and the structural characteristics of the resulting debris bed [1-2].

If the natural circulation is not sufficient in removing the decay heat produced by the debris, then dry-out, reheating and re-melting of the debris bed is expected to occur. In such a case, attack of molten core materials on the reactor containment basement presents a credible threat to containment integrity. The amount of heat which can be removed by the natural circulation coolant water inside the containment from the debris bed is depending among other factors, upon the properties of the bed as porous debris bed media. It is reported earlier [3] that debris agglomeration and especially formation of “cake” regions can significantly increase hydraulic resistance for the coolant flow and thus negatively affect coolability of the debris bed.

Many reports suggested that, if the melt is not completely solidified prior to settlement on top of the debris bed, then agglomeration of the debris and even “cake” formation is possible [4-9]. Many researchers have observed the formation of agglomeration of the debris particles and “cake” formation in fuel-coolant interaction (FCI) experiments with prototypic corium mixtures [4, 6, 7, 10] (e.g. in FARO [4, 10], CCM [6] and CWTI [7] tests) and with corium simulant materials (e.g. DEFOR-E [11] and DEFOR-S [9] tests). The most comprehensive information was presented in FARO tests [4, 10]. It suggests that the particle agglomeration

decreases as a function of the pool depth, however there exist a high uncertainty in the findings [12].

Debris agglomeration and ‘cake’ formation have been reported earlier in DEFOR tests [9, 11] in which sub-cooling of water was lower than 30°C and water pool depth was not sufficient to achieve complete solidification of the melt. Agglomerate can be defined as a lump of particles which are soldered together by liquid melt, although some individual particles can also be observed. A cake formation can be observed when no separate solid particles are distinguishable after solidification and the melt does not have open porosity for coolant ingress. A debris cake is basically a piece of solid melt with some shrinkage cavities. In debris cake formation, the fraction of liquid melt during solidification process will be quite large. The formation of particle agglomeration or cake is an unfavorable conditions as such high volume debris mass has very high heat capacities which may not be sufficiently cooled by the natural circulation of water inside the containment. Eventually, such adverse condition poses threat to the containment integrity and also chances of particle re-melt due to decay heat.

An experimental facility named MATE (Melt jet breakup Analysis with Thermal Effect) was set up at POSTECH, Korea, for the investigation of the jet breakup length and particle size distribution. The facility is capable of a gravitationally delivering melt jet (nozzle diameter of 14–35 mm) of metal alloy with low melting point into a water pool with a depth of 1.5 m. The melt jet behavior before its entry into the water, i.e., the jet diameter, jet velocity and fluctuation of the jet diameter was observed using high speed cameras. The influence of the estimation methods for the jet diameter and the jet breakup length on the uncertainty in the non-dimensional jet breakup length was reported in previous works [13-14]. Also, a comparison of the previous and present data, using a consistent analysis method, was provided.

Here, first systematic experimental research was conducted to study the particle size distribution and agglomerated debris using an interference grid for melt jet fragmentation. The test data is valuable for understanding of the basic phenomena and development of the models for melt jet fragmentation using

interference grid. Comparison of present data with previous work [4, 10] (FARO tests) is also presented

## 2. Test facility and instrumentation

Fig. 1 presents the schematic of the MATE facility. MATE facility consists of two parts: a water pool and a crucible for the melt jet generation and discharge. The water pool is a rectangular vessel with the cross sectional dimensions of 0.55m×0.55m (width×length) and a height of 2 m, and can heat water up to the saturation temperature at the ambient pressure. A steam generator is used to heat up the water pool upto saturation level. The main frame of the pool is made of stainless steel and polycarbonate plates that are attached for visualization. The crucible is made of stainless steel, and can melt a maximum load volume of 4 liters and reach a temperature of 350 °C.

A plug system and a slide gate system are used as nozzle opening system of the crucible. During the melting stage of the Bi-Sn alloy, the plug blocked the nozzle inside the crucible (Fig. 2) and the argon gas was injected continuously in order to prevent the oxidation of the melt. After the target melt temperature was reached, the experiments were commenced by pulling the plug upward using an air cylinder. The molten metal was then released into the water pool under the force of gravity, at the ambient pressure. The inlet of the melt release nozzle was designed with a bell mouth profile. The Bi-Sn alloy at the eutectic composition (58:42 wt%, melting temperature: 138 °C) was used as a simulant of corium. The Bi-Sn alloy has a density of 8750 kg/m<sup>3</sup> and a surface tension of approximately 0.4 N/m which are comparable to those of corium. The Bi-Sn alloy is more effective for the visualization than the high melting temperature materials, e.g. oxide materials. Since the Bi-Sn alloy has relatively lower temperature than corium, the water pool was heated to saturated temperature to simulate the intense vapor generation.

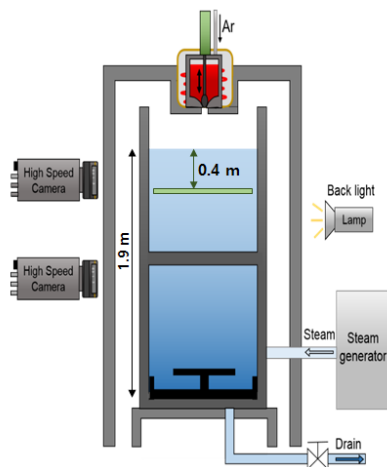


**Fig. 1:** Schematic design of MATE facility

Two high speed cameras and three video recorders are used for the visualization of experiments. One high

speed camera (lower) which covers the entire area of the water pool at 200–500 fps with a high resolution of approximately 0.5 mm/pixel is used for the measurement of the jet breakup length. Another high speed camera (upper) having a high resolution of approximately 0.25 mm/pixel was used to observe the smaller area near the water surface at 500–2000 fps for the measurement of the jet diameter and velocity before its entry into water. Before every test run, a calibration image was obtained with reference ruler using the lower high speed cameras before the ejection of melt. The reference ruler was positioned along the center axis of a water pool, where the melt jet flows down.

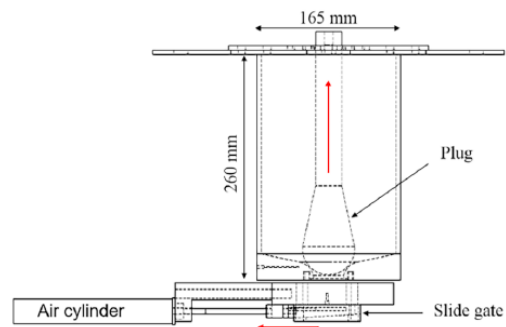
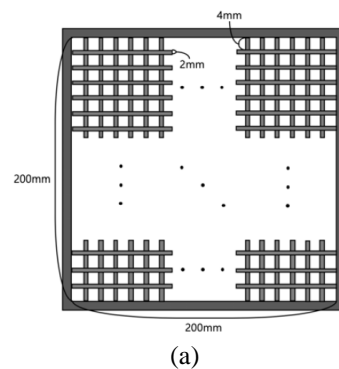


**Fig. 2:** Nozzle opening system plug and slide gate system



(a)



(b)

**Fig. 3:** (a) Mesh grid specification (b) mounting of grid in MATE tank

Fig. 3 (a) is a conceptual diagram of the underwater interference grid (mesh structure). Basically, it consists of a standardized mesh structure to be made using a SS-304 wire and a SS 304 frame. In the case of generally

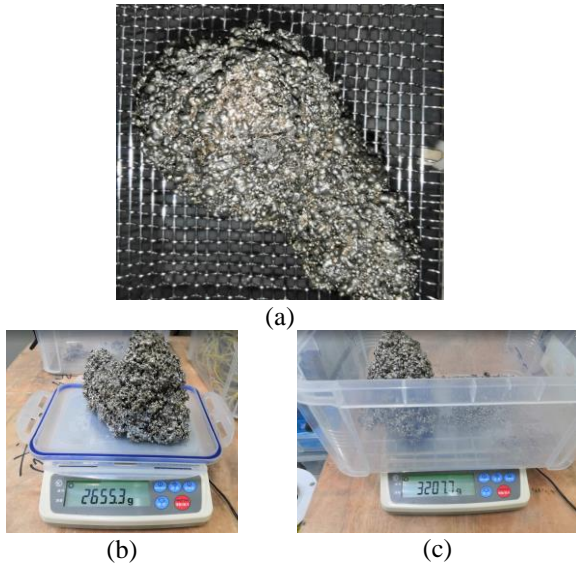
distributed commercial mesh, the thickness of the wire itself is thinner than the grid spacing. So in order to maintain the integrity of the grid according to contact with the high temperature melt and in consideration of the suitability of installation, the grid structure was made in house with the specification shown in Fig 3 (b). The spacing between the grids was maintained at 4 mm and a stainless steel wire having an outer diameter of 2 mm was used as a material for manufacturing the grid. Considering the size of the MATE tank and the size of the jet, the size of the grid structure was determined to be 200 mm in width and 200 mm in length. Under these conditions, the grid structure was designed so that approximately  $(200/(4+2) \sim 33)$  33 grid spaces were arranged in a line both horizontally and vertically.

### 3. Results and Discussion

#### 3.1 MATE-MM-1 test case (Failed test)

**Table 1:** Test case experimental conditions MATE-MM-1

Test case	Grid position (cm)	Pressure (bar)	Nozzle dia. (mm)	Melt Mass	Water Temperature
MM-1	15	2	14	4 kg	Saturated



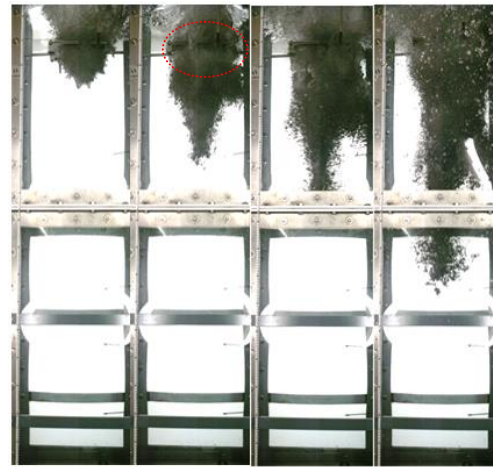
**Fig. 4:** (a) Agglomerated debris cake formation: Failed MATE MM - 1 tests (b) weight of MATE MM - 1 cake (c) total weight of MATE MM - 1

Table 1 lists the experimental conditions for the MATE-MM-1 test case. The failure of the slide gate system during MATE-MM-1 test resulted in a failed test case but it presented a very interesting observation. Due to the failure of the slide gate system, initially a very small orifice is available for liquid melt to pass through the crucible nozzle. It resulted in melt release in the form of droplets and patches rather than a continuous melt jet. Due to this, the melt droplets drops into the

tank and solidified over the grid as pressure was not sufficient enough to pass through the grid. After a certain time period the slide gate opened partially more and the size of the patches increases. Since the grid has been covered with solidified melt already, the incoming melts starts depositing over solidified debris over the grid and a cake formation is observed as shown in Fig. 4.

**Table 2:** Test case experimental conditions MATE-MM-2

Test case	Grid position (cm)	Pressure (bar)	Nozzle dia. (mm)	Melt Mass	Water Temp.
MM-2	15	2	14	10.4 kg	Saturated



(a)



(b)

(c)



(d)

**Fig. 5:** Snapshots of melt jet progression during MATE-MM-2 (b) debris particle sedimentation over grid (c) weight of the melt particles deposited over the grid (d) spreading pattern in the tank bottom

#### 3.2 MATE-MM-2 test case

Table 2 lists the experimental conditions for the MATE-MM-2 test case. For this case, higher melt mass was used. When the melt temperature reaches 300°C,

the plug and slide gates were actuated to open and allow the liquid melt to fall in the water tank. For this case, the force of the melt jet was high enough to pass through the grid as shown in Fig. 5 (a). High disturbance in the melt jet is observed after it passing from the grid. From the visual observation, it can be postulated that, jet breakup has been occurred near the region of the grid resulting in a very short jet breakup length compared to the previous study [13-14]. Fig. 5 (b) shows the solidified melt particles sedimentation on top of the grid. One can notice that the deposition of solidified debris particles over the grid is relatively smaller for MATE-MM-2 compared to MATE-MM-1. This is because the melt jet reaches the grid in a form of coherent jet rather than as liquid droplets. The solidified debris particles are carefully collected for measurement as shown in Fig. 5(c). Fig. 5(d) shows that the debris particles are uniformly distributed over the particle catcher plate with no visual agglomerated particles lump.

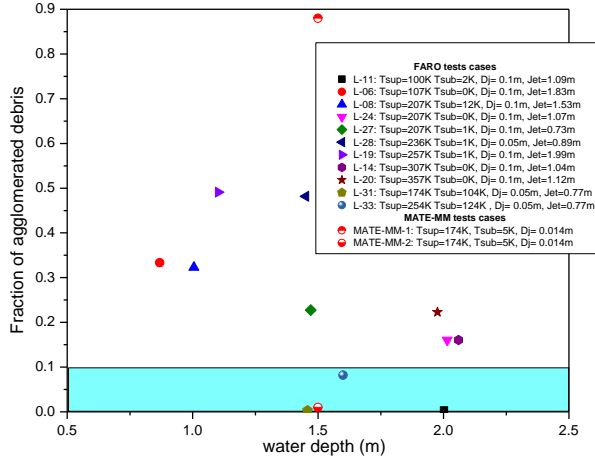


Fig. 6: Fraction of agglomerated debris in FARO and MATE-MM tests

The most comprehensive data up to date on agglomeration of prototypic corium mixtures is obtained in FARO tests [4, 10]. There are two data points (L-33 vs. L-28) which suggest that water sub-cooling is an important factor which can significantly reduce fraction of agglomerated debris at the same pool depth. While comparing the data points from MATE-MM-2 test case with FARO test data sets at similar pool depth of 1.5 m and water sub-cooling, i.e. L-27 and L-28, one can notice that the fraction of agglomerated debris particles has been significantly reduced due to the use of interference grid.

Fig. 7 shows the particle size distribution for MATE-MM-2 and its comparison with previous finds MATE - 10 [13]. It can be seen that the fraction of particle size above 4 mm is significantly lower. The lower particle sizes are favorable for cooling by natural circulation of water inside the containment.

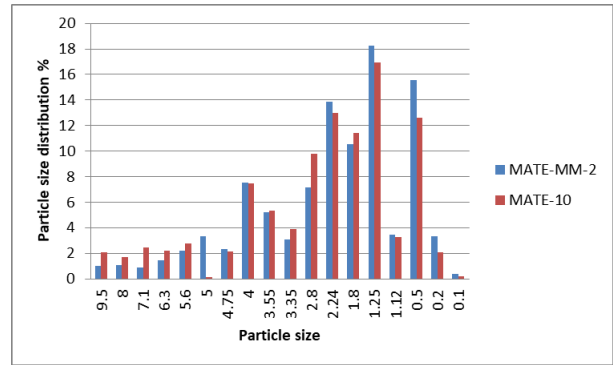


Fig. 7: Particle size distribution for MATE-MM-2 test case

#### 4. Conclusion

The MATE-MM tests provide first systematic experimental data about the particle size distribution and agglomerated debris using an interference grid for melt jet fragmentation. One of the main findings in the MATE-MM tests is that fraction of agglomerated debris above 5 mm reduced greatly. While a very small fraction of debris particles were found deposited over the grid. Also the fraction of agglomerated debris particles has been significantly reduced compared to previous work at similar pool depth due to the use of interference grid.

#### Acknowledgement

This work was supported by KOREA HYDRO & NUCLEAR POWER CO., LTD (No. 2018-RFP-Safety-5). Authors are thankful to Seokwon Whang from DANE, POSTECH for his assistance during experiments.

#### REFERENCES

- [1] Moriyama, K., Park, H.S., Hwang, B., Jung, W.H., 2016. Analysis of ex-vessel melt jet breakup and coolability. Part 1: sensitivity on model parameters and accident conditions. Nucl. Eng. Des. 302, 107–117.
- [2] Moriyama, K., Park, H.S., Hwang, B., Jung, W.H., 2016. Analysis of ex-vessel melt jet breakup and coolability. Part 2: uncertainty analysis. Nucl. Eng. Des. 302, 118–127.
- [3] Yakush, S., Kudinov, P., Dinh, T.-N., 2009. Multiscale simulations of self-organization phenomena in the formation and coolability of corium debris bed. In: Proceeding of NURETH-13, September 27–October 2, Kanazawa City, Ishikawa Prefecture, Japan, Paper N13P1143.
- [4] Magallon, D., Huhtiniemi, I., Hohmann, H., 1997. Lessons learnt from FARO/TERMO Scorium melt quenching experiments. In: Proceedings of the OECD/CSNI Specialists Meeting on Fuel-Coolant Interactions, Tokai-Mura, Japan, NEA/CSNI/R(97)26, Part II, pp. 431–446.
- [5] Spencer, B.W., Sienicki, J.J., McUumber, L.M., 1987. Hydrodynamics and Heat Transfer Aspects of Corium/Water Interactions. EPRI NP-5127. Electric Power Research Institute, Palo Alto, CA.
- [6] Spencer, B.W., Wang, K., Blomquist, C.A., McUumber, L.M., Schneider, J.P., 1994. Fragmentation and Quench Behaviour of Corium Melt Streams in Water. NUREG/CR-6133 ANL-93/32. Argonne National Laboratory.
- [7] Kudinov, P., Davydov, M., 2009. Development of ex-vessel debris agglomeration mode map for a LWR severe

- accident conditions. In: Proceedings of the 17th International Conference on Nuclear Engineering, Brussels, Belgium, July 12–16 (paper ICONE17-ICONE75080).
- [8] Kudinov, P., Davydov, M., 2009. Approach to prediction of melt debris agglomeration modes in a LWR severe accident. In: Proceedings of ISAMM-2009, Böttstein, Switzerland, October 26–28.
- [9] Kudinov, P., Davydov, M., 2010. Development and validation of the approach to prediction of mass fraction of agglomerated debris. In: Proceedings of 8th International Topical Meeting on Nuclear Thermal-Hydraulics, Operation and Safety (NUTHOS-8), Shanghai, China, October 10–14, Paper N8P0298.
- [10] Magallon, D., 2006. Characteristics of corium debris bed generated in large-scale fuel-coolant interaction experiments. Nucl. Eng. Des. 236, p.1998–p. 2009.
- [11] Karbojian, A., Ma, W., Kudinov, P., Dinh, T.-N., 2009. A scoping study of debris bed formation in the DEFOR test facility. Nucl. Eng. Des. 239, p.1653–p.1659.
- [12] Kudinov, P., Davydov, M., 2013. Development and validation of conservative-mechanistic and best estimate approaches to quantifying mass fractions of agglomerated debris. Nucl. Eng. Des. 262C, 452–461.  
<http://dx.doi.org/10.1016/j.nucengdes.2013.05.020>.
- [13] Jung, W.H., Park, H.S., Moriyama, K., Kim, M.H., 2019. Analysis of experimental uncertainties in jet breakup length and jet diameter during molten fuel-coolant interaction. 344, 183–194.
- [14] Jung, W.H., Park, H.S., Oh, J.H., Hwang, B., Lee, M., Kim, M.H., 2020. Minimum diameter limit of particle size distribution and its effect on coolability of debris bed. Nucl. Eng. Des., 110606.